PRODUCTION AND DECAYS OF STOPS, SBOTTOMS, AND STAUS

H. Eberl, S. Kraml, W. Majerotto
Inst. f. Hochenergiephysik der ÖAW,
Nikolsdorfer G. 18, A–1050 Vienna, Austria

A. Bartl, W. Porod
Inst. f. Theoretische Physik, Univ. Wien,
Boltzmanng. 5, A–1090 Vienna, Austria

We present a phenomenological analysis of production and decays of $\tilde{t}$, $\tilde{b}$, and $\tilde{\tau}$ in e^+e^- collisions with $\sqrt{s} = 500$ – 800 GeV. We include SUSY–QCD and Yukawa coupling corrections as well as initial state radiation. We show that e^- beam polarization is a powerful tool for a determination of the underlying SUSY parameters. Using in addition a polarized e^+ beam improves the precision of the parameter determination by about 25%.

1 Introduction

Supersymmetry (SUSY) implies the existence of two scalar partners $\tilde{q}_L$, $\tilde{q}_R$ (squarks) and $\tilde{\ell}_L$, $\tilde{\ell}_R$ (sleptons) to each quark q and lepton ℓ, respectively. The squarks and sleptons of the third generation are of special interest due to their sizeable Yukawa couplings being proportional to m_q or m_ℓ. These may induce a large mixing between $\tilde{f}_L$ and $\tilde{f}_R$ (with $\tilde{f} = \tilde{q}$ or $\tilde{\ell}$), $\tilde{f}_1 = \cos\theta_{\tilde{f}}\tilde{f}_L + \sin\theta_{\tilde{f}}\tilde{f}_R$, $\tilde{f}_2 = -\sin\theta_{\tilde{f}}\tilde{f}_L + \cos\theta_{\tilde{f}}\tilde{f}_R$, where $\tilde{f}_{1,2}$ are the mass eigenstates ($m_{\tilde{f}_1} < m_{\tilde{f}_2}$). In particular, the stop $\tilde{t}_1$ is most likely the lightest squark due to the large top mass. Also $\tilde{b}_1$ and $\tilde{\tau}_1$ can be relatively light for large $\tan\beta = v_2/v_1$ (where v_1 and v_2 are the vacuum expectation values of the two Higgs doublets). Hence these particles might be produced in e^+e^- collisions at the next linear collider with a center of mass energy $\sqrt{s} \gtrsim 500$ GeV. Their properties could be determined precisely enough to test supersymmetric models. In this contribution we want to give a rather complete phenomenological analysis of the production and decays of stops, sbottoms, and staus. In particular, we discuss the usefulness of polarisation of the e^- and e^+ beams for the determination of the underlying SUSY parameters.

2 Production cross section

At an e^+e^- collider, $\tilde{t}$, $\tilde{b}$, and $\tilde{\tau}$ can be pair–produced via γ and Z exchange in the s–channel. The total cross section shows the typical β^3 dependence, where β is the velocity of the outgoing sfermions. It has turned out that conventional QCD corrections[1,2] as well as SUSY–QCD corrections[3] and Yukawa coupling corrections[4] are important. Moreover, it is necessary to take into account initial state radiation[2] (ISR). As an example, we compare in Fig. 1 the $\sqrt{s}$ dependence of the tree level cross sections of $e^+e^- \to \tilde{t}_i\bar{\tilde{t}}_j$ and $e^+e^- \to \tilde{b}_i\bar{\tilde{b}}_j$ with the total (SUSY–QCD, Yukawa

coupling, and ISR) corrected cross sections for $m_{\tilde{t}_1} = 218$ GeV, $m_{\tilde{t}_2} = 317$ GeV, $\cos\theta_{\tilde{t}} = -0.64$, $m_{\tilde{b}_1} = 200$ GeV, $m_{\tilde{b}_2} = 278$ GeV, $\cos\theta_{\tilde{b}} = 0.79$, $M = 200$ GeV, $\mu = 1000$ GeV, $\tan\beta = 4$, and $m_A = 300$ GeV. Figure 2 shows the gluon, gluino, and Yukawa coupling corrections for $\tilde{t}_1\bar{\tilde{t}}_1$ and $\tilde{b}_1\bar{\tilde{b}}_1$ production relative to the tree level cross section for the parameters of Fig. 1. As can be seen, all three contributions can be significant for precision measurements. In the case of stau production, Yukawa coupling corrections are typically $\lesssim 5\%$. ISR changes the cross section by up to $\sim 25\%$.

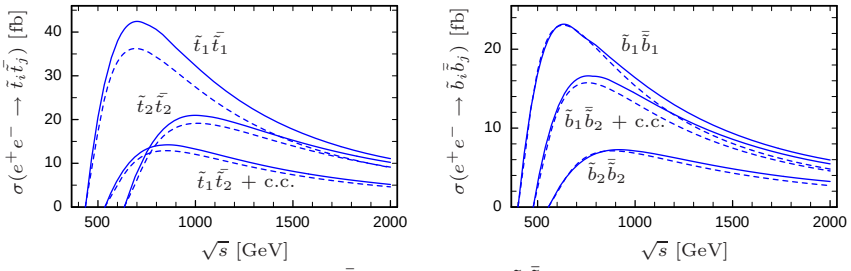

Figure 1: Cross sections for $e^+e^- \to \tilde{t}_i\bar{\tilde{t}}_j$ and $e^+e^- \to \tilde{b}_i\bar{\tilde{b}}_j$ as a function of $\sqrt{s}$ for $m_{\tilde{t}_1} = 218$ GeV, $m_{\tilde{t}_2} = 317$ GeV, $\cos\theta_{\tilde{t}} = -0.64$, $m_{\tilde{b}_1} = 200$ GeV, $m_{\tilde{b}_2} = 278$ GeV, $\cos\theta_{\tilde{b}} = 0.79$, $M = 200$ GeV, $\mu = 1000$ GeV, $\tan\beta = 4$, and $m_A = 300$ GeV; the dashed lines show the tree level and the full lines the total corrected cross sections.

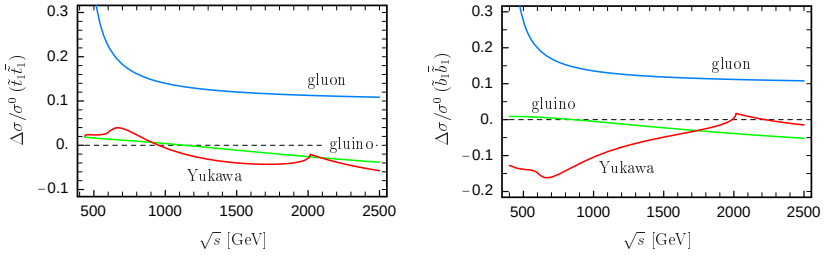

Figure 2: Gluon, gluino, and Yukawa coupling corrections [4] for $e^+e^- \to \tilde{t}_1\bar{\tilde{t}}_1$ and $e^+e^- \to \tilde{b}_1\bar{\tilde{b}}_1$ relative to the tree–level cross section for the parameters of Fig. 1.

Beam polarization can be used to enhance the signal and reduce the background. Figure 3 a shows $\sigma(e^+e^- \to \tilde{t}_1\bar{\tilde{t}}_1)$ in the $\mathcal{P}_-$–$\mathcal{P}_+$ plane, with $\mathcal{P}_-$ the polarization of the e^- beam and $\mathcal{P}_+$ that of e^+ beam ($\mathcal{P}_\pm = \{-1, 0, 1\}$ for {left–, un–, right–} polarized), for $m_{\tilde{t}_1} = 200$ GeV, $\cos\theta_{\tilde{t}} = -0.66$, and $\sqrt{s} = 500$ GeV. For the SUSY–QCD and Yukawa coupling corrections we have used $m_{\tilde{t}_2} = 420$ GeV, $m_{\tilde{b}_1} = 297$ GeV, $m_{\tilde{b}_2} = 345$ GeV, $\cos\theta_{\tilde{b}} = 0.84$, $M = 200$ GeV, $\mu = 800$ GeV, $m_A = 300$ GeV, and $\tan\beta = 4$. ISR has also been taken into account. The non–shaded area is the range of polarization of the TESLA design [5].

We next estimate the precision one may obtain for the stop parameters from cross section measurements. We use the parameter point of Fig. 3 a, i.e. $m_{\tilde{t}_1} = 200$ GeV, $m_{\tilde{t}_2} = 420$ GeV, $\cos\theta_{\tilde{t}} = -0.66$, etc. as an illustrative example: For 90% left–polarized electrons (and unpolarized positrons) we have $\sigma_L(\tilde{t}_1\bar{\tilde{t}}_1) = 44.88$ fb.

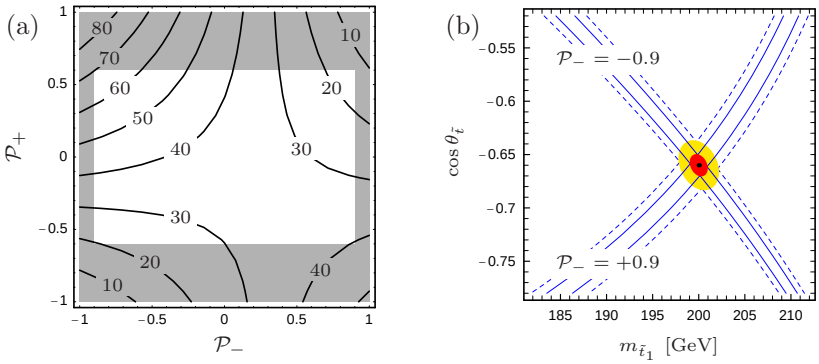

Figure 3: (a) Dependence of $\sigma(e^+e^- \to \tilde{t}_1\bar{\tilde{t}}_1)$ (in fb) on the beam polarization, for $m_{\tilde{t}_1} = 200$ GeV, $\cos\theta_{\tilde{t}} = -0.66$, $\sqrt{s} = 500$ GeV, and the other parameters as given in the text. (b) Error bands and 68% CL error ellipse for determining $m_{\tilde{t}_1}$ and $\cos\theta_{\tilde{t}}$ from cross section measurements, for $\mathcal{P}_- = \pm 0.9$, $\mathcal{P}_+ = 0$, and the other parameters as in (a); the dashed lines are for $\mathcal{L} = 100\,\text{fb}^{-1}$ and the full lines for $\mathcal{L} = 500\,\text{fb}^{-1}$.

For 90% right–polarized electrons we have $\sigma_R(\tilde{t}_1\bar{\tilde{t}}_1) = 26.95\,\text{fb}$. According to the Monte Carlo study of [6] one can expect to measure these cross sections with an error of $\Delta\sigma_L = \pm 2.1\,\%$ and $\Delta\sigma_R = \pm 2.8\,\%$ in case of an integrated luminosity of $\mathcal{L} = 500\,\text{fb}^{-1}$ (i.e. $\mathcal{L} = 250\,\text{fb}^{-1}$ for each polarization). Scaling these values to $\mathcal{L} = 100\,\text{fb}^{-1}$ leads to $\Delta\sigma_L = \pm 4.7\,\%$ and $\Delta\sigma_R = \pm 6.3\,\%$. Figure 3 b shows the corresponding error bands and error ellipses in the $m_{\tilde{t}_1}$ – $\cos\theta_{\tilde{t}}$ plane. The resulting errors on the stop mass and mixing angle are: $|\Delta m_{\tilde{t}_1}| = 2.2$ GeV, $|\Delta\cos\theta_{\tilde{t}}| = 0.02$ for $\mathcal{L} = 100\,\text{fb}^{-1}$ and $|\Delta m_{\tilde{t}_1}| = 0.98$ GeV, $|\Delta\cos\theta_{\tilde{t}}| = 0.01$ for $\mathcal{L} = 500\,\text{fb}^{-1}$. With the additional use of a 60% polarized e^+ beam these values can still be improved by $\sim 25\%$. At $\sqrt{s} = 800$ GeV also $\tilde{t}_2$ can be produced: $\sigma(\tilde{t}_1\bar{\tilde{t}}_2 + \text{c.c.}) = 8.75\,\text{fb}$ for $\mathcal{P}_- = -0.9$ and $\mathcal{P}_+ = 0$. If this cross section can be measured with a precision of $\pm 6\%$ this leads to $m_{\tilde{t}_2} = 420 \pm 8.3$ GeV. [a] If $\tan\beta$ and μ are known from other measurements this then allows one to determine the soft SUSY breaking parameters of the stop sector. Assuming $\tan\beta = 4 \pm 0.4$ leads to $M_{\tilde{Q}} = 298.2 \pm 7.3$ GeV and $M_{\tilde{U}} = 264.4 \pm 6.7$ GeV. In addition, assuming $\mu = 800 \pm 80$ GeV we get $A_t = 586.5 \pm 34.5$ (or -186.5 ± 34.5) GeV. The ambiguity in A_t exists because the sign of $\cos\theta_{\tilde{t}}$ can hardly be determined from cross section measurements. This may, however, be possible from measuring decay branching ratios or the stop–Higgs couplings.

A method to reconstruct the squark mass by the decay kinematics has been proposed in [7]. Though their analysis was performed for squarks of the 1st and 2nd generation it is also applicable to the 3rd generation, and a precision similar to the one presented here can be expected. A Monte Carlo study of stau production, with $\tilde{\tau}_1 \to \tau\tilde{\chi}_1^0$, was performed in [8]. They also give a method for the parameter

[a] Here note that $\tilde{t}_1\bar{\tilde{t}}_1$ is produced at $\sqrt{s} = 800$ GeV with an even higher rate than at $\sqrt{s} = 500$ GeV. One can thus improve the errors on $m_{\tilde{t}_1}$, $m_{\tilde{t}_2}$, and $\cos\theta_{\tilde{t}}$ by combining the information obtained at different energies. However, we will not do this in this study.

determination concluding that $m_{\tilde{\tau}_1}$ and $\theta_{\tilde{\tau}}$ could be measured within an error of few percent.

3 Decays

Stop, sbottoms, and staus can have quite complicated decay modes [9,10,11]. In addition to the decays into fermions, i.e. into chargino, neutralino or gluino:

$$\begin{array}{lll} \tilde{t}_i \to b\tilde{\chi}_j^+, & \tilde{t}_i \to t\tilde{\chi}_k^0, & \tilde{t}_i \to t\tilde{g}, \\ \tilde{b}_i \to t\tilde{\chi}_j^-, & \tilde{b}_i \to b\tilde{\chi}_k^0, & \tilde{b}_i \to b\tilde{g}, \\ \tilde{\tau}_i \to \nu_\tau \tilde{\chi}_j^-, & \tilde{\tau}_i \to \tau\tilde{\chi}_k^0, & \end{array} \tag{1}$$

$(i, j = 1, 2;\ k = 1...4)$ they may also decay into bosons, i.e. into a lighter sfermion plus a gauge or Higgs boson:

$$\begin{array}{ll} \tilde{t}_i \to \tilde{b}_j + (W^+,\, H^+), & \tilde{t}_2 \to \tilde{t}_1 + (Z^0,\, h^0,\, H^0,\, A^0), \\ \tilde{b}_i \to \tilde{t}_j + (W^-,\, H^-), & \tilde{b}_2 \to \tilde{b}_1 + (Z^0,\, h^0,\, H^0,\, A^0), \\ \tilde{\tau}_i \to \tilde{\nu}_\tau + (W^-,\, H^-), & \tilde{\tau}_2 \to \tilde{\tau}_1 + (Z^0,\, h^0,\, H^0,\, A^0), \end{array} \tag{2}$$

provided the mass splitting is large enough. If the 2–body decays (1) and (2) are kinematically forbidden, loop decays [1], 3–body [12], and even 4–body [13] decays come into play. For $\tilde{t}$ and $\tilde{b}$ decays SUSY–QCD corrections can be important [14,15,16,17]. In Fig. 4 we plot the decay width of $\tilde{t}_1 \to b\tilde{\chi}_1^+$ as a function of $\cos\theta_{\tilde{t}}$ for $m_{\tilde{t}_1} = 200$ GeV, $m_{\tilde{t}_2} = 490$ GeV, $m_{\tilde{\chi}_1^+} = 133$ GeV and $\tan\beta = 3$. Two cases are shown: one for $\tilde{\chi}_1^+ \sim \tilde{W}^+$ ($M \ll |\mu|$) and one for $\tilde{\chi}_1^+ \sim \tilde{H}^+$ ($M \gg |\mu|$). In this figure the decay $\tilde{t}_1 \to b\tilde{\chi}_1^+$ has practically 100% branching ratio except where the tree–level coupling vanishes. Figure 5 shows the decay branching ratios of $\tilde{t}_2$ decays as a function of $m_{\tilde{t}_2}$ for $m_{\tilde{t}_1} = 200$ GeV, $\cos\theta_{\tilde{t}} = 0.6$, $M = 180$ GeV, $m_A = 150$ GeV, $\tan\beta = 3$, $\mu = 300$, $A_t = A_b$, and $M_{\tilde{D}} = 1.1\, M_{\tilde{Q}}$. As can be seen, decays into bosons may have large branching ratios [10]. For the stau decays we choose $m_{\tilde{\tau}_1} = 250$ GeV, $m_{\tilde{\tau}_2} = 500$ GeV, and $m_{\tilde{\tau}_L} < m_{\tilde{\tau}_R}$. Figure 6 a shows the sum of the branching ratios of the bosonic $\tilde{\tau}_2$ decays, $\sum \mathrm{BR}[\tilde{\tau}_2 \to \tilde{\tau}_1 + (Z^0,\, h^0,\, H^0,\, A^0),\, \tilde{\nu}_\tau + (W^-,\, H^-)]$, in the A_τ–μ plane for $\tan\beta = 30$. Figure 6 b shows the $\tan\beta$ dependence of the individual $\tilde{\tau}_2$ branching ratios for $A_\tau = 800$ GeV and $\mu = 1000$ GeV. Here "Gauge/Higgs + X" refers to the sum of the gauge and Higgs boson modes. Quite generally, the decays of $\tilde{t}_2$, $\tilde{b}_i$, and $\tilde{\tau}_2$ into Higgs or gauge bosons can be significant in a large parameter region due to the Yukawa couplings and mixings $\tilde{t}$, $\tilde{b}$, and $\tilde{\tau}$.

4 Conclusions

We have presented a rather complete phenomenological study of production and decays of stops, sbottoms, and staus in e^+e^- annihilation with $\sqrt{s} = 500$ – 800 GeV. We have emphasized the advantage of using polarized e^- and e^+ beams for a better determination of the SUSY parameters. We have shown that at high luminosity ($\mathcal{L} \sim 500$ fb^{-1}) it is absolutely necessary to include SUSY–QCD and Yukawa coupling correction because the cross section can be measured at a few percent level.

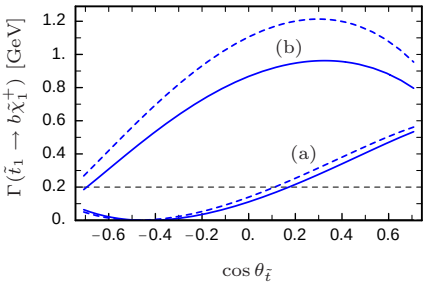

Figure 4: Decay width of $\tilde{t}_1$ as a function of $\cos\theta_{\tilde{t}}$ for $m_{\tilde{t}_1} = 200$ GeV, $m_{\tilde{t}_2} = 490$ GeV, $m_{\tilde{\chi}_1^+} = 133$ GeV and $\tan\beta = 3$; in (a) $M = 160$ GeV, $\mu = 300$ GeV and in (b) $M = 300$ GeV, $\mu = 160$ GeV. The dashed lines are the tree–level and the full lines the SUSY–QCD corrected results.

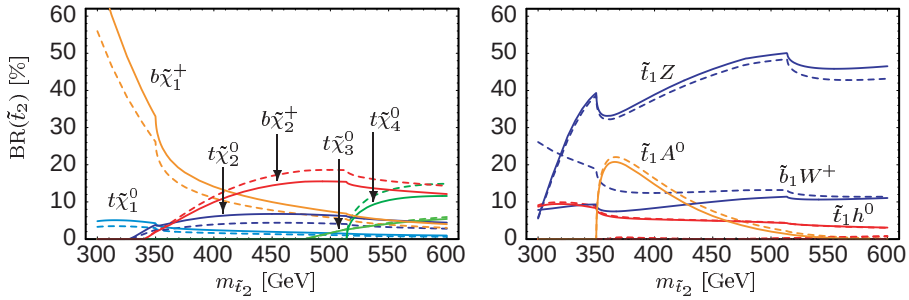

Figure 5: Branching ratios of $\tilde{t}_2$ decays as a function of $m_{\tilde{t}_2}$ for $m_{\tilde{t}_1} = 200$ GeV, $\cos\theta_{\tilde{t}} = 0.6$, $M = 180$ GeV, $m_A = 150$ GeV, $\tan\beta = 3$, $\mu = 300$ GeV, $A_t = A_b$, and $M_{\tilde{D}} = 1.1\, M_{\tilde{Q}}$; the dashed lines show the tree level and the full lines the SUSY–QCD corrected results.

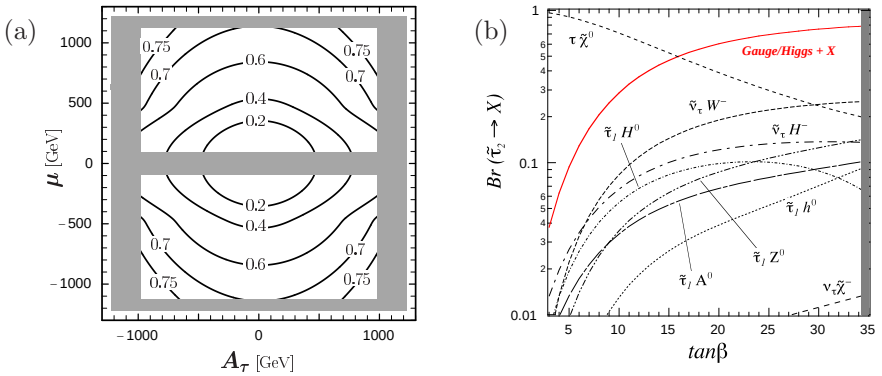

Figure 6: Branching ratios of $\tilde{\tau}_2$ decays for $m_{\tilde{\tau}_1} = 250$ GeV, $m_{\tilde{\tau}_2} = 500$ GeV, and $m_{\tilde{\tau}_L} < m_{\tilde{\tau}_R}$: (a) $\sum \mathrm{BR}[\tilde{\tau}_2 \to \tilde{\tau}_1 + (Z^0, h^0, H^0, A^0), \tilde{\nu}_\tau + (W^-, H^-)]$ for $\tan\beta = 30$; (b) $\tan\beta$ dependence of the individual branching ratios for $A_\tau = 800$ GeV and $\mu = 1000$ GeV; the other parameters are as in Fig. 5.

Acknowledgments

We thank K. Hidaka, T. Kon, and Y. Yamada for a fruitful collaboration. We are grateful to W. Adam for useful discussions. We thank H. Nowak and A. Sopczak for

clarifying correspondence. This work has been supported in part by the "Fonds zur Förderung der wissenschaftlichen Forschung" of Austria, project no. P13139–PHY.

References

1. K. I. Hikasa and M. Kobayashi, *Phys. Rev.* D **36**, 724 (1987).
2. M. Drees and K. I. Hikasa, *Phys. Lett.* B **252**, 127 (1990).
3. H. Eberl, A. Bartl and W. Majerotto, *Nucl. Phys.* B **472**, 481 (1996).
4. H. Eberl, S. Kraml and W. Majerotto, JHEP 9905 (1999) 016.
5. R. Brinkmann, 2nd ECFA/DESY Study on Physics and Detectors for a Linear Electron–Positron Collider, LAL Orsay, France, April 1998, `http://www.lal.in2p3.fr/Workshop/ECFA-DESY-LC98/`.
6. M. Berggren, R. Keränen, H. Nowak and A. Sopczak, *these proceedings*; H. Nowak, private communication.
7. J. L. Feng and D. E. Finnell, *Phys. Rev.* D **49**, 2369 (1994).
8. M. M. Nojiri, K. Fujii and T. Tsukamoto, *Phys. Rev.* D **54**, 6756 (1996)
9. A. Bartl, W. Majerotto and W. Porod *Z. Phys.* C **64**, 499 (1994), *Z. Phys.* C **68**, 518 (1995) (E).
10. A. Bartl, H. Eberl, K. Hidaka, S. Kraml, T. Kon, W. Majerotto, W. Porod and Y. Yamada, *Phys. Lett.* B **435**, 118 (1998).
11. A. Bartl, H. Eberl, K. Hidaka, S. Kraml, T. Kon, W. Majerotto, W. Porod and Y. Yamada, `hep-ph/9904417`, to appear in *Phys. Lett.* B.
12. W. Porod and T. Wöhrmann, *Phys. Rev.* D **55**, 2907 (1997); W. Porod, *Phys. Rev.* D **59**, 095009 (1999).
13. C. Boehm, A. Djouadi and Y. Mambrini, `hep-ph/9907428`.
14. W. Beenakker, R. Höpker and P. M. Zerwas, *Phys. Lett.* B **378**, 159 (1996); W. Beenakker, R. Höpker, T. Plehn and P. M. Zerwas, *Z. Phys.* C **75**, 349 (1997).
15. S. Kraml, H. Eberl, A. Bartl, W. Majerotto and W. Porod, *Phys. Lett.* B **386**, 175 (1996); A. Djouadi, W. Hollik and C. Jünger, *Phys. Rev.* D **55**, 6975 (1997).
16. A. Bartl, H. Eberl, K. Hidaka, S. Kraml, W. Majerotto, W. Porod and Y. Yamada, *Phys. Lett.* B **419**, 243 (1998).
17. A. Arhib, A. Djouadi, W. Hollik and C. Jünger, *Phys. Rev.* D **57**, 5860 (1998); A. Bartl, H. Eberl, K. Hidaka, S. Kraml, W. Majerotto, W. Porod and Y. Yamada, *Phys. Rev.* D **59**, 115007 (1999).